MOLECULAR PHARMACOLOGY
Vol. 69, No. 3
16170/3087795
Printed in U.S.A.

Mol Pharmacol 69:1007–1014, 2006

Electrophysiological Characterization of Benzofuroindole-Induced Potentiation of Large-Conductance Ca^{2+}-Activated K^+ Channels

Tal Soo Ha,[1] Hyun-Ho Lim, Ga Eun Lee, Yong-Chul Kim, and Chul-Seung Park

Department of Life Science, Gwangju Institute of Science and Technology, Gwangju, Korea

Received June 28, 2005; accepted December 6, 2005

ABSTRACT

Large-conductance Ca^{2+}-activated K^+ (BK_{Ca}) channels are widely distributed and play key roles in various cell functions. We previously reported the chemical synthesis of several benzofuroindole compounds that act as potent openers of BK_{Ca} channels. In this study, we investigated the mechanism of channel potentiation by one of the compounds, 7-trifluoromethyl-10*H*-benzo[4,5]furo[3,2-*b*]indole-1-carboxylic acid (TBIC), using electrophysiological means. This chemical highly activated cloned BK_{Ca} channels from extracellular side independent of β subunits and regardless of the presence of intracellular Ca^{2+}. The EC_{50} and Hill coefficient for rat BK_{Ca} channel α subunit, rSlo, were estimated as 8.9 ± 1.5 μM and 0.9, respectively. TBIC shifted the conductance-voltage curve of rSlo channels to more hyperpolarized potentials without altering its voltage dependence. Single-channel recording revealed that TBIC increased the open probability of the channel in a dose-dependent manner without any changes in single-channel conductance. Strong potentiation by TBIC was also observed for native BK_{Ca} channels from rat hippocampus pyramidal neurons. Thus, TBIC and the related benzofuroindole compounds can be useful tools to unravel the mechanism of this novel allosteric activation of BK_{Ca} channels.

Large-conductance Ca^{2+}-activated K^+ channels (BK_{Ca} or maxi-K channels) are a family of potassium-selective ion channels activated in response to membrane depolarization and are modulated by intracellular concentration of Ca^{2+} (for reviews, see Toro et al., 1998; Weiger et al., 2002). These channels are widely expressed in many different types of both excitable and nonexcitable cells. They have significant physiological roles in regulation of frequency of firing, action potential afterhyperpolarization, and neurotransmitter release (Vergara et al., 1998; Kaczorowski and Garcia, 1999). Their activities play a pivotal role in the negative feedback control of intracellular Ca^{2+} concentration and protect neuronal cells from excess Ca^{2+} influx through the voltage-dependent Ca^{2+} channels during pathophysiological environments (Lawson, 2000). In hyperactive neuronal cells, activation of BK_{Ca} channels is thought to be required for restoring resting membrane potential by down-regulating the activity of voltage-dependent Na^+ and Ca^{2+} channels (Brenner et al., 2000; Jaggar et al., 2000). In addition, activation of BK_{Ca} channel significantly contributes to action potential repolarization and afterhyperpolarization during excitation-contraction coupling in smooth muscle cells (Ohi et al., 2001).

For these reasons, BK_{Ca} channel openers may be effective in protecting neuronal cells from damage during or after ischemic stroke and in down-regulating hyperactivity in smooth muscle cells (for review, see Shieh et al., 2000). BK_{Ca} channels are composed of two different subunits: the pore-forming α subunit and the auxiliary β subunits. Although channels formed only by four α subunits can be functional, β subunits alter the biophysical and pharmacological properties of homomeric channels, including Ca^{2+} and voltage sensitivity, and gating kinetics (Valverde et al., 1999; Wallner et al., 1999; Xia et al., 1999; Qian et al., 2002; Ha et al., 2004). Several compounds have been developed and reported to be

This research was supported by grant R01-2002-000-00354-0 from Korea Science and Technology Foundation and grant 21C Frontier, 03K2201-00320 from the Ministry of Science and Technology of Korea (to C.-S.P.) and grant Korea Health 21 R&D Project, 0405-NS01-0704-0001-13 from the Ministry of Health and Welfare (to Y.-C.K.).

[1] Current affiliation: Department of Pharmacology and Center for Basic Neuroscience, University of Texas Southwestern Medical Center, Dallas, Texas.

Article, publication date, and citation information can be found at http://molpharm.aspetjournals.org.
doi:10.1124/mol.105.016170.

ABBREVIATIONS: BK_{Ca}, large-conductance Ca^{2+}-activated K^+ channel; TBIC, 7-trifluoromethyl-10*H*-benzo[4,5]furo[3,2-*b*]indole-1-carboxylic acid; rSlo, rat BK_{Ca} channel α subunit; hβ1, human β1 subunit of BK_{Ca} channel; rβ4, rat β4 subunit of BK_{Ca} channel; I-V, current-voltage; G-V, conductance-voltage; NS-1619, 1,3-dihydro-1-(2-hydroxy-5-(trifluoromethyl)phenyl)-5-(trifluoromethyl)-2*H*-benzimidazol-2-one; BMS-204352, (3*S*)-3-(5-chloro-2-methoxyphenyl)-3-fluoro-6-(trifluoromethyl)-1,3-dihydro-2*H*-indol-2-one.

BK_{Ca} channel openers (e.g., dehydrosoyasaponin-I, maxikdiol, NS-1619, BMS-204352, 17β-estradiol, ethylbromide tamoxifen, pimaric acid, and epoxyeicosatrienoic acids) (Vergara et al., 1998; Valverde et al., 1999; Coghlan et al., 2001; Dick et al., 2002; Imaizumi et al., 2002). Although some synthetic activators, such as NS-1619 and BMS-204352, act on the α subunit, other openers of BK_{Ca} channels, including dehydrosoyasaponin-I and 17-β-estradiol, require β subunit for their action (Giangiacomo et al., 1998; Valverde et al., 1999). Several activators derived from natural products such as dehydrosoyasaponin-I are impermeable to the cell membrane and act only on intracellular side of BK_{Ca} channels (Kaczorowski and Garcia, 1999).

Benzofuroindole analogs were shown to relax smooth muscles of bladder possibly via the activation of BK_{Ca} channels (Butera et al., 2001). In our previous study, we reported the chemical synthesis of new benzofuroindole derivatives and the screening for their efficacy on cloned BK_{Ca} channels expressed in *Xenopus laevis* oocytes (Gormemis et al., 2005). One of the initial compounds, referred to as "compound 8," highly up-regulated the activity of BK_{Ca} channels. In the present study, we further investigated this compound, 7-trifluoromethyl-10*H*-benzo[4,5]furo[3,2-*b*]indole-1-carboxylic acid (TBIC) (Fig. 1, inset), to reveal its mechanism of action with respect to channel activation. We found that TBIC activated BK_{Ca} channel in a dose-dependent manner at micromolar concentration from extracellular side and its activation was independent of β subunits. TBIC shifted the conductance-voltage relationship of the channel to more hyperpolarized potentials without altering voltage dependence. In addition, single-channel analysis showed that the compound increased the open probability (P_o) of the channel by altering gating kinetics without affecting its single-channel conductance.

Materials and Methods

Functional Expression of Cloned BK_{Ca} Channel Subunits in *X. laevis* Oocytes. The cDNAs of rat BK_{Ca} channel α subunit (rSlo), human β1 subunit (hβ1), and rat β4 subunit (rβ4) were subcloned into pGH vector for expression in *X. laevis* oocytes. The sequence information of rSlo, hβ1, and rβ4 used in this study are listed with GenBank under the accession numbers AF135265 (Ha et al., 2000), NM004137 (Meera et al., 1996), and AY028605 (Ha et al., 2004), respectively. Each cDNA was subcloned into pGH expression vector containing the 5′- and 3′-untranslated regions of *X. laevis* β-globin gene, because it is known to enhance the protein expression of certain mammalian messages in *X. laevis* oocytes (Liman et al., 1992). cRNA of each construct was prepared in vitro as described in previous studies (Ha et al., 2000, 2004). Plasmid DNA was purified (midi-prep columns; QIAGEN, Valencia, CA) and digested with a restriction enzyme, NotI. RNA was synthesized from linearized plasmid DNA using T7 RNA polymerase in the presence of a cap analog, m7G(5′)ppp(5′)G, and NTPs. Oocytes of stages V to VI were surgically removed from the ovarian lobes of anesthetized female *X. laevis* frogs (Xenopus I, Dexter, MI) and transferred into Ca^{2+}-free OR medium (86 mM NaCl, 1.5 mM KCl, 2 mM $MgCl_2$, 10 mM HEPES, and 50 μg/ml gentamicin at pH 7.6). The follicular cell layer was removed by incubating oocytes in Ca^{2+}-free OR medium containing 3 mg/ml collagenases (Worthington Biochemicals, Freehold, NJ) for 2 h. The oocytes were then washed extensively with and kept in ND-96 medium (96 mM NaCl, 2 mM KCl, 1.8 mM $CaCl_2$, 1 mM $MgCl_2$, 5 mM HEPES, and 50 μg/ml gentamicin at pH 7.6) at 18°C. Each oocyte was injected with 50 nl containing approximately 1 ng of cRNA for single-channel and 50 ng for macroscopic current recordings, respectively, using a microdispenser (Drummond Scientific, Broomall, PA). Injected oocytes were incubated at 18°C for 3 to 5 days in sterile ND-96 medium. Immediately before patch-clamp experiments, the vitelline membrane was removed manually with fine forceps.

Primary Culture of Pyramidal Neurons in Rat Hippocampus. Primary culture of rat hippocampal pyramidal neuron has been described previously (Abdel-Hamid and Baimbridge, 1997). Sprague-Dawley rats were anesthetized and decapitated at embryonic day 18. The hippocampus was surgically dissected and isolated from fetal brain and minced in Ca^{2+}, Mg^{2+}-free Hanks' balanced salt solution (Invitrogen, Carlsbad, CA). The tissue was digested with 0.1% trypsin-EDTA to the medium and then stopped by adding the same volume of fetal bovine serum. Cell dissociation was accomplished by gentle mechanical agitation. After removing cell debris by centrifugation for 2 min, the cell pellet was resuspended in minimal essential medium (Invitrogen) with 10% of a 1:1 mixture of heat-inactivated horse and fetal bovine serum. The dissociated cells were plated on 35-mm tissue culture dishes (Falcon; BD Biosciences Discovery Labware, Franklin Lakes, NJ) coated with poly-L-lysine (Sigma-

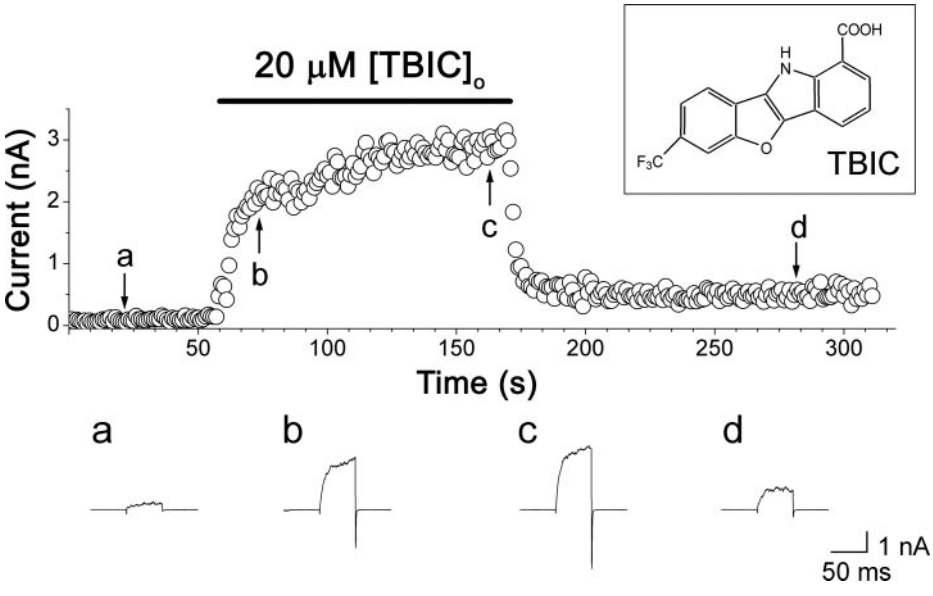

Fig. 1. Rapid and reversible activation of macroscopic rSlo channel currents by TBIC. Representative diary-plot of mean currents evoked by rSlo channels was shown as a continuous recording. Ionic currents were elicited every second with 50-ms step-pulses of 50 mV from the holding voltage of −100 mV. Currents were averaged for 3 ms in between 45 to 48 ms of voltage pulse. TBIC was superfused on extracellular side of patch membrane at 20 μM (solid bar). Each representative current trace (a–d) was obtained at the time indicated by arrows. Inset, chemical structure of TBIC.

Aldrich, St. Louis, MO). The cells were incubated at 37°C in a humidified, 5% CO_2 incubator. The medium was renewed after 24 h and half-exchanged twice a week with feeding media. The feeding media contained apo-transferrin (200 μg/ml; Sigma-Aldrich), insulin (1 μg/ml; Sigma-Aldrich), sodium selenite (30 nM; Sigma-Aldrich), putrescine (100 μM; Sigma-Aldrich), progesterone (20 μM; Sigma-Aldrich), 5% equine serum (Hyclone Laboratories, Logan, UT), and minimal essential medium (Invitrogen). The cultured neurons were used for electrophysiological recording during 12 to 18 days in culture.

Electrophysiological Recordings and Data Analysis. All single-channel and macroscopic current recordings were performed using gigaohm-seal patch-clamp method in either excised inside-out or outside-out configuration (Hamil et al., 1981). Patch pipettes were fabricated from borosilicate glass (WPI, Sarasota, FL) and fire-polished to the resistance of 2 to 5 MΩ for macroscopic patches and 5 to 8 MΩ for single-channel recording, respectively. For single-channel recordings, patch pipettes were coated with beeswax to reduce electrical noise. The channel currents were amplified using an Axopatch 200B amplifier (Axon Instruments, Foster City, CA), low-pass filtered at 1 or 2 kHz using a four-pole Bessel filter, and digitized at a rate of 10 or 20 points/ms using a Digidata 1200A (Axon Instruments). No series resistance compensation was used and linear leak currents were subtracted from macroscopic currents.

In recording rat hippocampal neurons, pyramidal cells were distinguished from mixed population including glia by morphological features. Before electrophysiological recording, the culture medium was washed multiple times with Na^+-saline solution containing 140 mM NaCl, 4 mM KCl, 0.24 mM KH_2PO_4, 2 mM $MgCl_2$, 2 mM $CaCl_2$, 10 mM D-glucose, and 10 mM HEPES, pH 7.4. Cells were then rinsed in symmetrical 124 mM K^+ solution for recordings. Patch recordings were made from the soma of cultured pyramidal neurons in the outside-out patch configuration at room temperature. From a total of 76 patches in neuron cells, 22 recordings showed single-channel level activities of BK_{Ca} channels

Single rSlo or native BK_{Ca} channels were readily activated at high concentration of intracellular Ca^{2+} and by briefly delivered membrane potentials to 100 mV. For single-channel analysis, transitions between closed and open states were determined by setting the threshold at half of the unitary current amplitude. To determine the single-channel conductance of expressed channels, mean amplitudes of channel currents were obtained from histograms fitted with Gaussian distributions, and the mean currents were plotted against transmembrane voltages. Slope-conductance values were obtained from linear regression.

Macroscopic currents of expressed channels were activated by voltage-clamp pulses delivered from a holding potential of −50 mV for $[Ca^{2+}]_i$ at 0 μM, −100 mV at 1 μM, and −150 mV at 5 μM, respectively, to membrane potentials ranging usually from −150 to 200 mV in 10- or 20-mV increments. Solutions for both single- and macroscopic channel recordings contained gluconates as a nonpermeant anion to prevent the activation of endogenous calcium-activated chloride channels. The intracellular and extracellular solutions contained the following components unless specified otherwise: 120 mM potassium gluconate, 10 mM HEPES, 4 mM KCl, and 5 mM EGTA, pH 7.2. To provide required free $[Ca^{2+}]_i$, the appropriate amount of total Ca^{2+} to add to the intracellular solution was calculated using the program MaxChelator (Patton et al., 2004; http://www.standford.edu/~cpatton/maxc.html). To compare the channel characteristics accurately, an identical set of intracellular solutions was used throughout the entire experiments. Commercial software packages, such as Clampex 8.0 or 8.1 (Axon Instruments) and Origin 6.1 (OriginLab Corp., Northampton, MA), were used for the acquisition and the analysis of both single-channel and macroscopic recording data.

Reagents. The chemical synthesis of TBIC was described in a previous study where the compound was referred to as "compound 8" (Gormemis et al., 2005). TBIC was dissolved in dimethyl sulfoxide (Sigma-Aldrich) in 500 mM stock solutions and stored at −20°C until use. All reagents, buffered in bath solution to pH 7.2, were applied directly to membrane patches by gravity perfusion with 10 volumes of recording chamber at a flow rate of 1 to 2 ml/min.

Statistical Analysis. All data were presented as means ± S.E.M., where n indicates the number of independent experiments. For each data set, the statistical significance of the difference was tested using analysis of variance for independent observations. In all cases, $P < 0.05$ was considered significant. Each macroscopic current trace represents an average of three records in succession.

Results

Effects of TBIC, a Benzofuroindole, on Macroscopic Currents of a Cloned BK_{Ca} Channel Expressed in *X. laevis* Oocytes. To understand the potentiation mechanism of TBIC on BK_{Ca} channels, we first characterized its effects on macroscopic currents of rat BK_{Ca} channel α subunit (rSlo) expressed in *X. laevis* oocytes. As shown in Fig. 1, the time-dependent effects of TBIC were monitored from a membrane patch containing hundreds of rSlo channels by applying 50-ms step-pulses to 50 mV every second. Small rSlo currents were initially evoked by the voltage pulses (Fig. 1a), because the intracellular (pipette) solution contained only 0.5 μM Ca^{2+}. When 20 μM TBIC was applied on to the extracellular side of membrane patch, a large increase in the rSlo currents was observed. The full potentiation was achieved in two phases: the initial fast-activation occurring within 10 s (Fig. 1b) and the following slower phase over a few minutes (Fig. 1c). Upon cessation of TBIC application, the channel activity rapidly decreased within in 10 s (Fig. 1d). In some cases, the channel activity did not return fully to the pretreatment level, and a slight increase in channel activity remained (Fig. 1, a and d). However, the fast onset and offset of TBIC effects in cell-free recording condition suggest strongly that the compound interacts directly with the channel from extracellular side and enhances its activity.

Concentration Dependence of TBIC on Macroscopic rSlo Channels and Effects of β Subunits. We then determined the concentration dependence of TBIC on macroscopic rSlo currents. As increasing concentrations of TBIC were applied to the extracellular side of membrane patches, the activation rate as well as the level of steady-state current was increased in a concentration-dependent manner (Fig. 2A). To compare the effects of TBIC measured at specific concentrations, we normalized the ionic currents in the presence of a given concentration of TBIC (I) with the current in the absence of TBIC (I_0). The relative -fold increase (I/I_0) was plotted against the concentration of TBIC and fitted with a Hill equation (Fig. 2A, right). Although we were not able to obtain a concentration of TBIC higher than 300 μM because of its solubility in water, we noticed that TBIC-induced current increases reached plateau levels at around 100 μM (Fig. 2A). The half-effective concentration (EC_{50}) and Hill coefficient (n) were obtained by fitting individual titration data to Hill equation (Fig. 2 legend), and the statistical means and standard errors were calculated using the values obtained from more than three independent experiments. The EC_{50} and n of extracellular TBIC for rSlo channels were determined as 8.9 ± 1.5 μM and 0.9 ± 0.1, respectively (Fig. 2A, ●; $n = 5$). We also measured the effects of TBIC using inside-out patch configuration to determine whether this compound also affects channel activity from the intracellular side. The

intracellular Ca^{2+} concentration was fixed at 2 μM to activate rSlo channels, and different concentrations of TBIC were added to the intracellular side of the membrane. Although intracellular TBIC also increased rSlo currents with a similar apparent affinity, EC_{50} of 12.7 ± 5.8 μM, its -fold increase was much smaller than that obtained from extracellular side (Fig. 2A, ■; $n = 3$).

The functional characteristics of BK_{Ca} channels are altered by auxiliary β subunits, and the efficacy of some activators and inhibitors is greatly influenced by coassembly of β subunits. Thus, we asked whether the potentiating effects of TBIC are affected by coexpression of β subunits. We expressed rSlo together with either human β1 or rat β4 subunit in *X. laevis* oocytes and measured the channel currents in the presence of different concentrations of extracellular TBIC. We usually used 12-fold molar excess of the hβ1 and rβ4 transcripts to ensure the sufficient coassembly of β subunits with rSlo subunit. The activities of both rSlo/hβ1 (Fig. 2B; $n = 4$) and rSlo/rβ4 (Fig. 2C; $n = 4$) were increased by micromolar concentration of the compound in a concentration-dependent manner. EC_{50} values of extracellular TBIC were determined as 10.0 ± 1.5 μM for rSlo/hβ1 heteromeric channels (Fig. 2B, ▲) and 4.5 ± 0.7 μM for rSlo/rβ4 heteromeric channels (Fig. 2C, ♦) with Hill coefficients of 0.7 ± 0.1 and 1.1 ± 0.2, respectively, indicating that minor but statistically significant differences in both the apparent affinity and the cooperativity of TBIC were produced by the coexpression of different β subunits. However, these results indicate that TBIC can potentiate BK_{Ca} channel without the coassembly of β subunits and argue that the receptor site of TBIC locates within the main subunit of BK_{Ca} channel, the Slo protein.

Efficacy of Extracellular TBIC in Different Concentrations of Intracellular Ca^{2+}. Because the activity of BK_{Ca} channels is modulated by intracellular Ca^{2+}, we wondered how intracellular Ca^{2+} interplay affects the action of TBIC from the extracellular side and whether TBIC can activate channel in the absence of intracellular Ca^{2+}.

We tested the effects of extracellular TBIC at two different concentrations in the absence of intracellular Ca^{2+} (Fig. 3A). To keep $[Ca^{2+}]_i$ in the subnanomolar range, 5 mM EGTA was supplemented into the intracellular pipette solution. Even in the absence of intracellular Ca^{2+}, the activation of rSlo channels was observed at extreme positive voltages, greater 100 mV (top row, control). The application of 30 μM extracellular TBIC greatly potentiated the channel activity, and large outward currents were measured (top row, 30 μM $[TBIC]_o$). As illustrated in the current-voltage (I-V) relationship (top row, right), TBIC shifted the threshold voltage of channel activation to less positive voltages, and the channel currents were observed at voltages as low as 60 mV in 30 μM TBIC (○). In the presence of 100 μM TBIC, I-V relationship of rSlo channel was further shifted, and the currents were activated near 20 mV (△). Robust outward currents were consistently recorded at the membrane voltages greater than 20 mV. In the presence of 1 μM $[Ca^{2+}]_i$, 30 μM TBIC also shifted the I-V relationship to less positive voltages, and large tail currents evoked by rSlo were observed (middle row, 30 μM $[TBIC]_o$). Because the channels were activated near −60 mV in the presence of 100 μM TBIC, we were able to detect inward currents at negative test-voltages (middle row, 100 μM $[TBIC]_o$; right, half-filled triangles). Inward currents were even more dramatic when $[Ca^{2+}]_i$ was increased to 5 μM (Fig. 3A, bottom row). With the treatment of 30 μM TBIC, the activation of rSlo channel became evident even at −100 mV, and the peak inward K^+ currents was observed at around −40 mV (●). The most impressive effect of TBIC was seen at 100 μM in the presence of 5 μM $[Ca^{2+}]_i$. rSlo channels were activated robustly from −130 mV, and resulted in large inward currents that peaked near −70 mV (bottom row, 100 μM $[TBIC]_o$; right, ▲). It is intriguing that the linear I-V relationship, a characteristic of the BK_{Ca} channel, could be appreciated by measuring steady-state currents instead of instantaneous tail currents.

The effects of TBIC on macroscopic rSlo channel are summarized in Fig. 3, B and C. Sets of conductance-voltage (G-V)

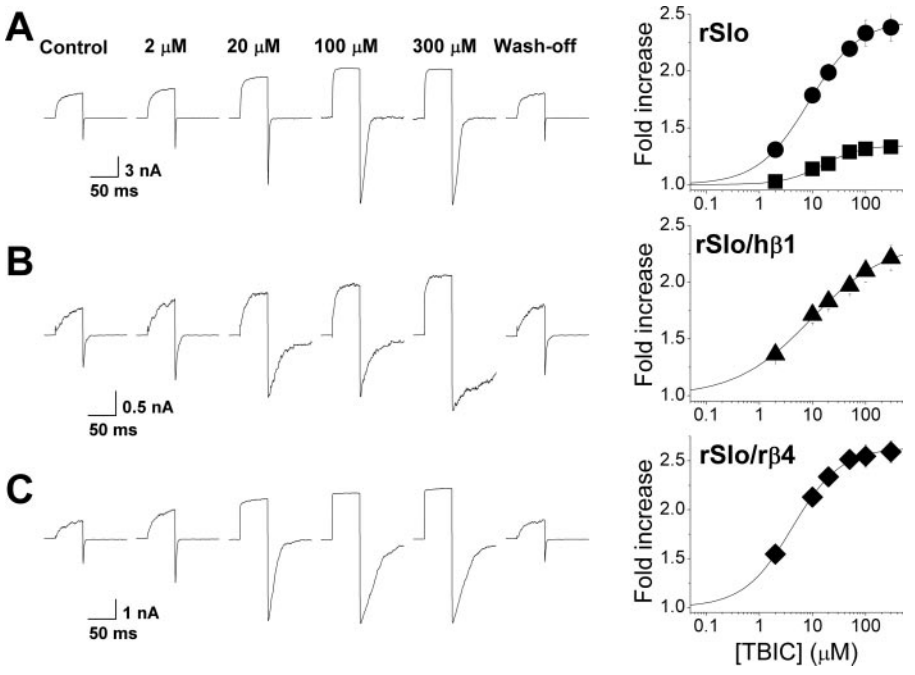

Fig. 2. Effects of β subunits on TBIC-dependent potentiation of macroscopic rSlo currents. Titration curves (right) of rSlo (A), rSlo/hβ1 (B), and rSlo/rβ4 channels (C) were shown with their representative raw traces in various TBIC concentrations (left). Ionic currents were elicited with 50-ms step-pulses of 50 ms from a holding voltage of −100 mV. Concentrations of extracellular TBIC are as indicated, and concentration of intracellular Ca^{2+} was fixed at 2 μM. The EC_{50} and n were obtained by fitting the experimental data to a logistic function, $I_{max} - I = (I_{max} - I_0)/\{1 + ([TBIC]/EC_{50})^{nH}\}$, derived from Hill equation, where I_0 and I_{max} represent the current in the absence of TBIC and the maximum current measured at 300 μM, respectively. The statistical of means and standard errors were calculated using the values obtained from more than three independent experiments. Although the titration curves of both extracellular (●) and intracellular TBIC (■) are shown for rSlo channel, only extracellular titrations are presented for rSlo/hβ1 (▲) and rSlo/rβ4 (♦). Each data point represents the mean ± S.E.M. of more than four independent recordings.

relationships and their half-activation voltages ($V_{1/2}$) were shown for four different concentrations of TBIC—0 μM (squares), 10 μM (circles), 30 μM (triangles), and 100 μM (inverted triangles)—in the presence of three different concentrations of $[Ca^{2+}]_i$: 0 μM (open), 1 μM (half-filled), and 5 μM (filled). The significant effects of TBIC on G-V relationship were observed at the concentrations higher than 1 μM, and the further increase resulted in steady shifts in G-V curves toward the negative direction. Although the addition of TBIC up to 100 μM shifted the G-V curve -134 mV, from 210 $\pm$ 7.5 to 76 $\pm$ 4.0 mV, in the absence of Ca^{2+}, a smaller shift of approximately -83 mV was observed by identical concentration of TBIC at 5 μM $[Ca^{2+}]_i$. Despite the large shifts in their positions, no significant change was detected in the steepness of G-V curves, the measure of voltage dependence in channel activation, within a set of identical $[Ca^{2+}]_i$. These results indicate that BK_{Ca} channel can be activated by TBIC in the absence of intracellular Ca^{2+} and that the potentiation is because of the shift of its voltage-activation profile to a more negative range without affecting its voltage sensitivity.

Effects of Extracellular TBIC on Single-Channel Currents of rSlo. To obtain further insight into the mechanism of action, the effects of TBIC were investigated at the single-channel level. For each outside-out patch, we depolarized the membrane voltage to more than 80 mV to significantly activate rSlo channels to count the number of channels in the membrane. Only those patches containing a single rSlo channel were used for subsequent experiments. Single-channel recordings were performed at various durations to obtain accurate values of steady-state kinetic constants: 5 to 8 min at hyperpolarized voltages and 0.5 to 2 min at depolarized voltages. Representative traces of a single rSlo channel in the absence and the presence of 20 μM TBIC were shown in Fig. 4A. The channel currents were recorded at 2 μM $[Ca^{2+}]_i$ at the specified membrane voltages. The opening of the channel was highly dependent on the membrane voltages as expected. The gating behavior, however, was dramatically altered by the application of 20 μM TBIC to the extracellular side (Fig. 4A). Although the rSlo channel rarely opens in control solution at -25 mV, the addition of 20 μM TBIC to the extracellular side made the channel open readily. In addition, P_o was greatly increased at 25 mV by TBIC treatment. To examine the effects of TBIC on single-channel conductance, we measured the unitary current amplitudes of rSlo at various membrane voltages in the absence and presence of TBIC, and the single-channel I-V relationships were plotted (Fig. 4B). Single-channel conductances

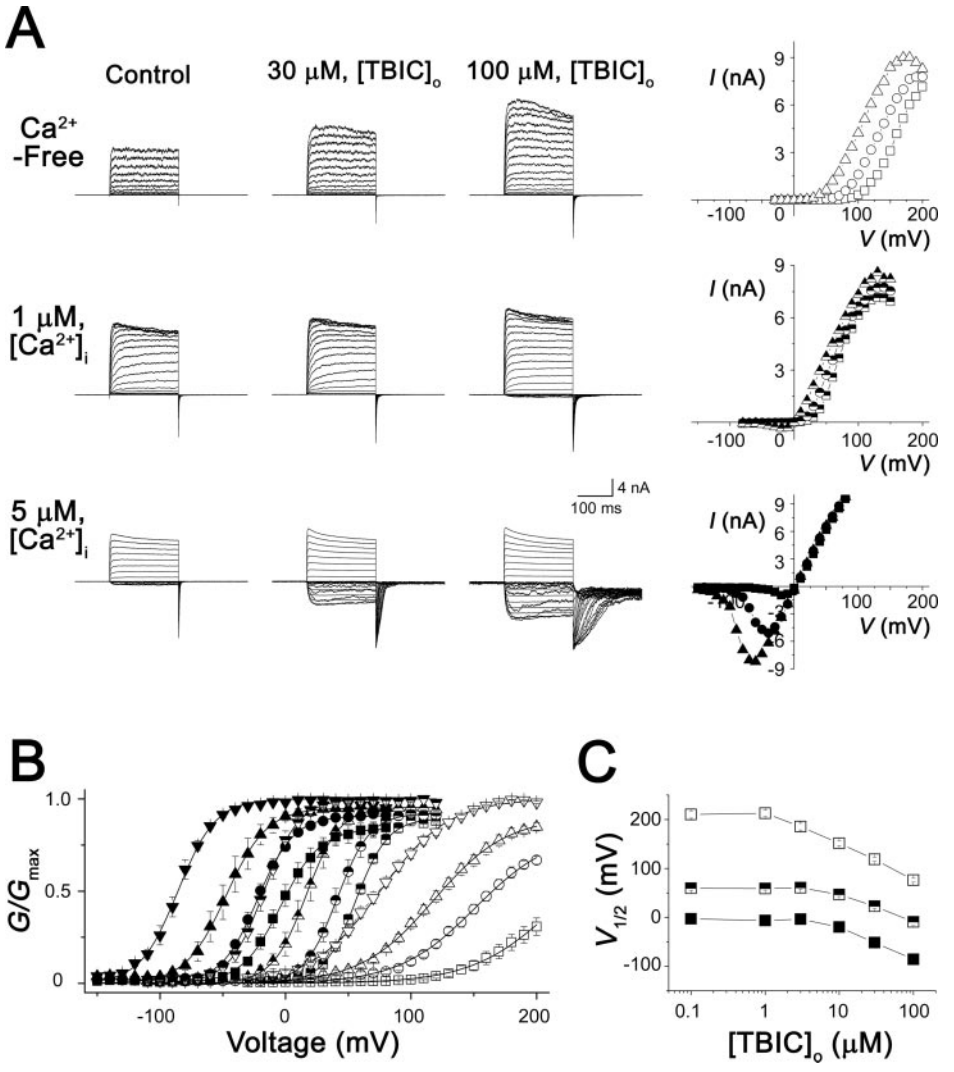

Fig. 3. Effects of TBIC on current-voltage and conductance-voltage relationships of macroscopic rSlo current. A, effects of TBIC on the macroscopic I-V relationship of rSlo in different $[Ca^{2+}]_i$. Representative current traces of macroscopic rSlo currents (left) and their I-V relationships (right) are shown for two different $[TBIC]_o$, 30 and 100 μM, and three different $[Ca^{2+}]_i$, Ca^{2+}-free (top), 1 μM (middle), and 5 μM (bottom). Ionic currents were elicited with 200-ms step-pulses of different voltage protocols: -30 to 200 mV in 10-mV increments at free calcium, -80 to 150 mV at 1 μM $[Ca^{2+}]_i$, and -150 to 80 mV at 5 μM $[Ca^{2+}]_i$ from holding potentials of -50, -100, and -150 mV, respectively. Each data point in I-V relationships represents the mean current value measured over 198 $\pm$ 1.5 ms of test pulses. The filling of symbols represents different concentrations of Ca^{2+}, Ca^{2+}-free (open), 1 μM (half-filled), and 5 μM (filled), the shape of the symbols indicates the concentration of TBIC: control or 0 μM (squares), 30 μM (circles), and 100 μM (triangles). B, effects of TBIC on the G-V relationships of macroscopic rSlo currents. Conductance values were obtained from peak tail currents and normalized to the maximum conductance observed at 100 μM $[TBIC]_o$. Each symbol represents the conductance values obtained from four different $[TBIC]_o$, control or 0 μM (squares), 10 μM (circles), 30 μM (triangles), and 100 μM (inverted triangles), and from three different $[Ca^{2+}]_i$; Ca^{2+}-free (open; $n = 6$), 1 μM (half-filled; $n = 4$), and 5 μM (filled; $n = 4$). C, effects of TBIC on $V_{1/2}$. Each data point represents the mean value $\pm$ S.E.M. of $V_{1/2}$ values obtained by fitting independent data sets with Boltzmann function. Symbols are as defined in B.

were estimated as 246.1 ± 5.4 pS in control and 247.7 ± 4.2 pS in TBIC, respectively, indicating that the drug did not affect the single-channel conductance of rSlo. We then analyzed the effects of TBIC on single-channel P_o of the channel. Under control conditions, the increase in P_o was highly dependent on membrane voltage in the range of −75 and 25 mV, and P_o values were well fitted by a Boltzmann function (Fig. 4C, open symbols). The voltage required for half-maximum activation, $V_{1/2}$, was determined as 38.1 ± 3.1 mV. In the presence of 20 μM TBIC, the P_o versus voltage curve shifted in a parallel manner to the negative direction by 33 mV and $V_{1/2}$ was estimated as 4.8 ±3.4 mV. It is worth noting that the slopes of voltage activation curve remained unchanged, 0.031 for control currents and 0.035 for TBIC-potentiated currents, respectively. These results are in a good agreement with the previous findings in macroscopic rSlo currents, where the G-V curve was also shifted in parallel by TBIC (Fig. 3B) further indicating that the potentiation of BK_{Ca} channel activity by TBIC is the direct result of the P_o increase.

Effects of TBIC on Single BK_{Ca} Channels of Cultured Hippocampus Pyramidal Neuron. Because BK_{Ca} channels in brain neurons are known to express as a heterogenous population because of extensive RNA splicing, coassembly with β4 subunit, and post-translational modifications, we wondered whether the activity of native neuronal BK_{Ca} channels could also be potentiated by TBIC. We thus performed outside-out patch recording on pyramidal neurons of rat hippocampus. Although in most instances more than one BK_{Ca} channels was observed in single patches, we were able to determine unambiguously the number of channels using brief depolarizing pulses. Representative current traces, obtained from a membrane patch containing four neuronal BK_{Ca} channels, were shown in Fig. 5. Similar to the single-channel recordings of rSlo channel expressed in *X. laevis* oocytes (Fig. 4A), neuronal BK_{Ca} channel showed high single-channel conductances and steep voltage dependence. Although extracellular treatment of 20 μM TBIC highly increased the P_o of native BK_{Ca} channels at all membrane voltages tested, the effects were more dramatic for negative voltage ranges. Although channel openings were observed only rarely in control solution containing 2 μM $[Ca^{2+}]_i$ at −25 mV, the opening of all four BK_{Ca} channels were frequently observed in the presence of 20 μM TBIC. The time-dependent effects of TBIC on neuronal BK_{Ca} channels were compared at two different voltages, 25 and −25 mV (Fig. 5, B and C). The P_o increase induced by TBIC treatment was almost instantaneous and readily reversible. Thus, we can conclude that this compound highly potentiates native BK_{Ca} channels from rat hippocampal neurons as well as the cloned rSlo channel.

Discussion

In the present study, we characterized the effects of a benzofuroindole derivative, TBIC, on BK_{Ca} channels. This compound highly activates both native and cloned BK_{Ca} channels in a dose-dependent manner from the extracellular side of the membrane at low micromolar concentrations. TBIC potentiates the channel activity by shifting its P_o-voltage relationship to more negative voltages without affecting the single-channel conductance or the voltage sensitivity. However, the action of TBIC is noncooperative, and thus the dose-response curve of TBIC is best fitted with Hill coefficient of 1.

TBIC is a derivative of benzofuroindole with a carboxylic acid and a trifluoromethyl moiety at the position 1 and 7, respectively (Fig. 1, inset). In our previous study, we showed that a negative charge at the position 1 and a strong electron-withdrawing group at the position 7 are critical for the activity of TBIC (Gormemis et al., 2005). Because TBIC acts

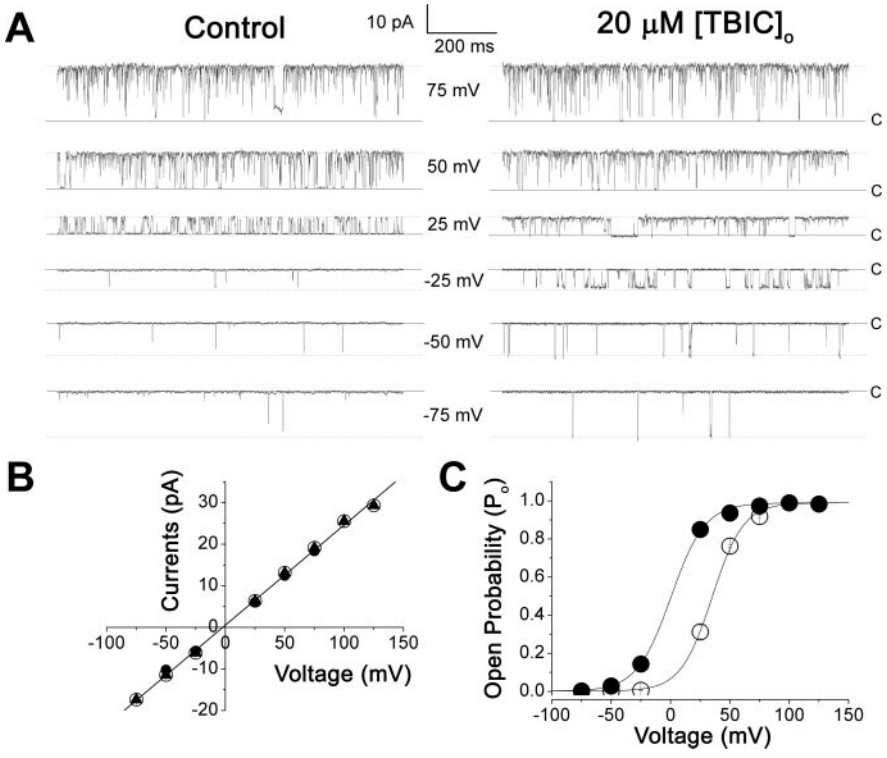

Fig. 4. Effect of TBIC on single rSlo channels. A, typical single-channel current recordings of rSlo channels were shown at different membrane voltages. The concentration of intracellular Ca^{2+} (pipette Ca^{2+} concentration) fixed at 2 μM. Ionic currents of single channels in a patch of oocyte membrane were continuously recorded at different membrane voltages in the absence (left) and presence of 20 μM TBIC perfused on the extracellular side (right). Open and closed states were denoted with dashed lines and solid lines (denoted as C), respectively. B, effects of TBIC on the single-channel conductance. The unitary current-amplitude determined at 2 μM intracellular Ca^{2+} in the absence (○; $n = 7$) or presence of 20 μM TBIC (●; $n = 5$) was plotted as a function of the test voltages. Each data point was obtained from all-points amplitude histograms fitted with Gaussian function. The slope-conductance of rSlo channel was estimated by linear least square regression. C, effects of TBIC on voltage-dependent P_o of single rSlo channel. Relationship of open probability against membrane voltages of single rSlo channel was plotted in the absence (○; $n = 5$) or presence of 20 μM TBIC (●; $n = 4$). Data points were individually fitted to Boltzmann equation ($P_o = [1/(1 + \exp\{(V_{1/2} - V)/k\}])$ (solid lines), and the slope factors (k) were determined as 0.031 for control and 0.035 for TBIC-induced currents, respectively. The open probability of single rSlo channel was determined at 2 μM $[Ca^{2+}]_i$.

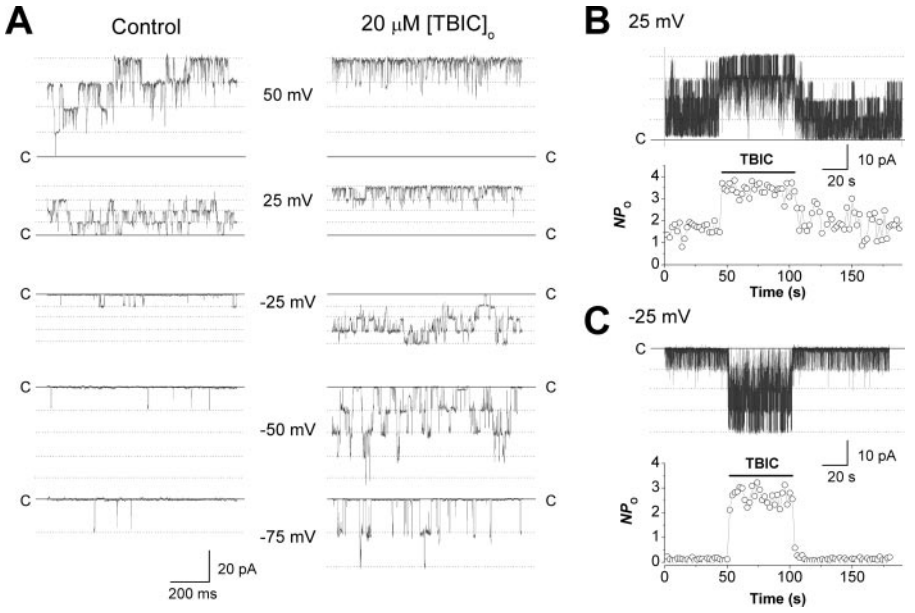

Fig. 5. Effect of TBIC on native BK_{Ca} channels from rat hippocampus pyramidal neuron. A, representative current traces of neuronal BK_{Ca} channels, recorded in excised outside-out membrane, were shown in the absence and the presence of TBIC at different membrane voltages. The intracellular free Ca^{2+} concentration was fixed at 2 μM and extracellular TBIC was fixed at 20 μM. Closed state and different open states were marked as a solid line (denoted as C) and dotted lines, respectively. Four BK_{Ca} channels were in this particular patch. The time-dependent effects of TBIC on native BK_{Ca} channels are shown in continuous recordings (top), and their P_o changes were monitored (bottom) at two different holding voltages, 25 mV (B) and −25 mV (C). P_o values were calculated in 2-s intervals, and the exposed time to extracellular TBIC is shown as a solid bar.

from extracellular side of the membrane and does not require β subunit for its action, we assume that the binding site of this negatively charged compound is in the extracellular region of the main subunit, Slo protein. The binding sites have not been identified for the previously known BK_{Ca} channel activators, especially those targeting the α subunit, such as NS-1619 and BMS-204352 (for reviews, see Starrett et al., 1996; Coghlan et al., 2001). Therefore, it remains unclear whether benzofuroindoles act on the identical site for their action. Thus, it is our desire to localize the receptor site for benzofuroindoles and to understand the molecular mechanism of this novel modulation. Slo protein, the α subunit of BK_{Ca} channel, has seven membrane-spanning regions (S0–S6) with an amino terminus of approximately 8 kDa and three loops facing the extracellular side of the membrane. The β1 subunit confers its potentiating effect by interacting with the extracellular N terminus and the first transmembrane helix, S0. Therefore, it is conceivable that the TBIC may interact with the same region and activates the channel activity (Meera et al., 1997; Cox and Aldrich, 2000; Dick et al., 2001). It remains to be seen whether the deletion of the N-terminal region removes the effect of TBIC. There has been much progress in predicting optimum binding site of a given compound based on detailed structure-activity relationship (Dick et al., 2001). The structure-activity profiles of benzofuroindole derivatives, reported in the previous studies (Butera et al., 2001; Gormemis et al., 2005), can be used to predict the potential sites for TBIC on BK_{Ca} channel α subunit.

TBIC can activate native neuronal BK_{Ca} channels as well as the heterologously expressed Slo channels. At the single-channel level, the compound never failed to potentiate the BK_{Ca} channels in excised membrane of cultured neuron. We noticed that the potentiating effects of TBIC on neuronal BK_{Ca} channel might be even greater than those on cloned BK_{Ca} channel, although we were not able to quantify this precisely. This variability might be the result of the splicing variants of Slo or post-translational modification of BK_{Ca} channels in specific neurons. In a previous report, benzofuroindole derivatives were described to activate BK_{Ca} channels of smooth muscles only in rat bladder but not in arteries (Butera et al., 2001). Because the efficacy of TBIC was not significantly affected by different β subunits (Fig. 2, B and C), we wonder whether differential splicing of the Slo message affects the efficacy of TBIC on BK_{Ca} channels in different tissues. Thus, it will be important to assess the effects of TBIC in BK_{Ca} channels in different tissues and to correlate the efficacy with the nature of BK_{Ca} channels in the future.

In conclusion, our results provide the mechanistic details of benzofuroindole action on BK_{Ca} channel as a potentiator. Because TBIC and related compounds can activate BK_{Ca} channels so effectively, they can be used as experimental probes for a new allosteric site important for channel activation and be served as lead compounds for developing synthetic activators of BK_{Ca} channel for pharmaceutical purposes.

Acknowledgments

We are grateful to the members of Laboratory of Molecular Neurobiology (Gwangju Institute of Science and Technology) for valuable comments and timely help throughout the work and to M. Walden (Brandeis University. Waltham, MA) for critical reading of the manuscript.

References

Abdel-Hamid KM and Baimbridge KG (1997) The effects of artificial calcium buffers on calcium responses and glutamate-mediated excitotoxicity in cultured hippocampal neurons. *Neuroscience* **81:**673–687.

Brenner R, Perez GJ, Bonev AD, Eckman DM, Kosek JC, Wiler SW, Patterson AJ, Nelson MT, and Aldrich RW (2000) Vasoregulation by the beta1 subunit of the calcium-activated potassium channel. *Nature (Lond)* **407:**870–876.

Butera JA, Antane SA, Hirth B, Lennox JR, Sheldon JH, Norton NW, Warga D, and Argentieri TM (2001) Synthesis and potassium channel opening activity of substituted 10H-benzo[4,5]furo[3,2-*b*]indole-and 5,10-dihydro-indeno[1,2-*b*]indole-1-carboxylic acids. *Bioorg Med Chem Lett* **11:**2093–2097.

Coghlan MJ, Carroll WA, and Gopalakrishnan M (2001) Recent developments in the biology and medicinal chemistry of potassium channel modulators: update from a decade of progress. *J Med Chem* **44:**1627–1653.

Cox DH and Aldrich RW (2000) Role of the beta1 subunit in large-conductance Ca^{2+}-activated K^+ channel gating energetics. Mechanisms of enhanced Ca^{2+} sensitivity. *J Gen Physiol* **116:**411–432.

Dick GM, Hunter AC, and Sanders KM (2002) Ethylbromide tamoxifen, a membrane-impermeant antiestrogen, activates smooth muscle calcium-activated large-conductance potassium channels from the extracellular side. *Mol Pharmacol* **61:** 1105–1113.

Dick GM, Rossow CF, Smirnov S, Horowitz B, and Sanders KM (2001) Tamoxifen

activates smooth muscle BK channels through the regulatory beta 1 subunit. *J Biol Chem* **276:**34594–34599.
Giangiacomo KM, Kamassah A, Harris G, and McManus OB (1998) Mechanism of maxi-K channel activation by dehydrosoyasaponin-I. *J Gen Physiol* **112:**485–501.
Gormemis AE, Ha TS, Im I, Jung KY, Lee JY, Park CS, and Kim YC (2005) Benzofuroindole analogues as potent BK_{Ca} channel openers. *Chembiochem* **6:**1745–1748.
Hamil OP, Marty A, Neher E, Sakmann B, and Sigworth FJ (1981) Improved patch-clamp techniques for high-resolution current recording from cells and cell-free membrane patches. *Pflueg Arch Eur J Physiol* **391:**85–100.
Ha TS, Heo MS, and Park CS (2004) Functional effects of auxiliary β4 subunit on rat large-conductance Ca^{2+}-activated K^+ channel. *Biophys J* **86:**2871–2882.
Ha TS, Jeong SY, Cho SW, Jeon H, Roh GS, Choi WS, and Park CS (2000) Functional characteristics of two BK_{Ca} channel variants differentially expressed in rat brain tissues. *Eur J Biochem* **267:**910–918.
Imaizumi Y, Sakamoto K, Yamada A, Hotta A, Ohya S, Muraki K, Uchiyama M, and Ohwada T (2002) Molecular basis of pimarane compounds as novel activators of large-conductance Ca^{2+}-activated K^+ channel α-subunit. *Mol Pharmacol* **62:**836–846.
Jaggar JH, Porter VA, Lederer WJ, and Nelson MT (2000) Calcium sparks in smooth muscle. *Am J Physiol* **278:**C235–C256.
Kaczorowski GJ and Garcia ML (1999) Pharmacology of voltage-gated and calcium-activated potassium channels. *Curr Opin Chem Biol* **3:**448–458.
Lawson K (2000) Is there a role for potassium channel openers in neuronal ion channel disorders? *Expert Opin Investig Drugs* **9:**2269–2280.
Liman ER, Tytgat J, and Hess P (1992) Subunit stoichiometry of a mammalian K^+ channel determined by construction of multimeric cDNAs. *Neuron* **9:**861–871.
Meera P, Wallner M, Jiang Z, and Toro L (1996) A calcium switch for the functional coupling between alpha (hslo) and beta subunits (KV,Ca beta) of maxi K channels. *FEBS Lett* **382:**84–88.
Meera P, Wallner M, Song M, and Toro L (1997) Large conductance voltage- and calcium-dependent K^+ channel, a distinct member of voltage-dependent ion channels with seven N-terminal transmembrane segments (S0–S6) and extracellular N terminus and an intracellular (S9–S10) C terminus. *Proc Natl Acad Sci USA* **94:**14066–14071.
Ohi Y, Yamamura H, Nagano N, Ohya S, Muraki K, Watanabe M, and Imaizumi Y (2001) Local Ca^{2+} transients and distribution of BK channels and ryanodine receptors in smooth muscle cells of guinea-pig vas deferens and urinary bladder. *J Physiol (Lond)* **534:**313–326.
Patton C, Thomson S, and Epel D (2004) Some precautions in using chelators to buffer metals in biological solutions. *Cell Calcium* **35:**427–431.
Qian X, Nimigean CM, Niu X, Moss BL, and Magleby KL (2002) Slo1 tail domains, but not the Ca^{2+} bowl, are required for the β1-subunit to increase the apparent Ca^{2+} sensitivity of BK channels. *J Gen Physiol* **120:**829–843.
Shieh CC, Coghlan M, Sullivan JP, and Gopalakrishnan M (2000) Potassium channels: molecular defects, diseases and therapeutic opportunities. *Pharmacol Rev* **52:**557–594.
Starrett JE, Dworetzky SI, and Gibkoff VK (1996) Modulators of large-conductance calcium-activated potassium (BK) channels as potential therapeutic targets. *Curr Pharm Des* **2:**413–428.
Toro L, Wallner M, Meera P, and Tanaka Y (1998) Maxi-K_{Ca}, a unique member of the voltage-gated K^+ channel superfamily. *News Physiol Sci* **13:**112–117.
Valverde MA, Rojas P, Amigo J, Cosmelli D, Orio P, Bahamonde MI, Mann GE, Vergara C, and Latorre R (1999) Acute activation of Maxi-K channels (hSlo) by estradiol binding to the beta subunit. *Science (Wash DC)* **285:**1929–1931.
Vergara C, Latorre R, Marrion NV, and Adelman JP (1998) Calcium-activated potassium channels. *Curr Opin Neurobiol* **8:**321–329.
Wallner M, Meera P, and Toro L (1999) Molecular basis of fast inactivation in voltage and Ca^{2+}-activated K^+ channels: a transmembrane β-subunit homolog. *Proc Natl Acad Sci USA* **96:**4137–4142.
Weiger TM, Hermann A, and Levitan IB (2002) Modulation of calcium-activated potassium channels. *J Comp Physiol A Neuroethol Sens Neural Behav Physiol* **188:**79–87.
Xia XM, Ding JP, and Lingle CJ (1999) Molecular basis for the inactivation of Ca^{2+}- and voltage-dependent BK channels in adrenal chromaffin cells and rat insulinoma tumor cells. *J Neurosci* **19:**5255–5264.

Address correspondence to: Dr. Chul-Seung Park, Department of Life Science, Gwangju Institute of Science and Technology, 1 Oryrong-dong, Bukgu, Gwangju, 500-712, Korea. E-mail: cspark@gist.ac.kr